Synergistic Lethality Effects of ABT-199 and Apatinib on DLBCL: Antitumor Efficacy and Underlying Mechanisms

Yuanfei Shi
Zhejiang University First Affiliated Hospital Department of Hematology
Jing Ye
Third Hospital of Beijing University: Peking University Third Hospital
Huafei Shen
Zhejiang University First Affiliated Hospital Department of Hematology
Yi Xu
Zhejiang University First Affiliated Hospital Department of Hematology
Rui Wan
Taihe Hospital
Xiujin Ye
Zhejiang University First Affiliated Hospital Department of Hematology
Jie Jin
Zhejiang University First Affiliated Hospital Department of Hematology
Wanzhuo Xie (xiewanzhuo@zju.edu.cn)
Zhejiang University School of Medicine First Affiliated Hospital

Research

Keywords: ABT-199, Apatinib, BCL-2, VEGFR2, EDN1, DLBCL, MAPK

Posted Date: November 10th, 2021

DOI: https://doi.org/10.21203/rs.3.rs-1013076/v1

Abstract

Background

To investigate the effect of ABT-199 combined with Apatinib on diffuse large B-cell lymphoma (DLBCL).

Methods

We explored the synergistic effect of ABT-199 and Apatinib in diffuse large B-cell lymphoma (DLBCL) cell lines, DLBCL patient samples, and DLBCL mouse models, using viability assay and immunoblotting. RNA sequencing assay helped identify mechanisms of ABT-199 plus Apatinib.

Results

ABT-199 combined with Apatinib inhibited cell proliferation, reduced colony-forming capacity, and induced apoptosis and cell cycle arrest in DLBCL cells. Mechanistically, the combination therapy inhibited tumor cell growth and promoted tumor cell death by regulating EDN1 and MAPK related pathways and activating the intrinsic apoptotic pathway. The effect of the combination therapy was also validated in primary DLBCL blasts and xenograft mouse models.

Conclusion

Our findings indicate that simultaneously targeting both BCL-2 and VEGFR2 might serve as a promising therapeutic strategy for DLBCL.

Introduction

Diffuse large B-cell lymphoma (DLBCL), the most common type of B-cell lymphoid malignancies in adults, is a genetically heterogeneous disease, which can be divided into indolent, aggressive, and highly invasive subtypes[1–4]. According to studies of gene expression profiling (GEP), DLBCL can be divided into germinal center B cell (GCB) and activated B cell (ABC) subtypes[5–7].

About 40% of DLBCL patients are characterized by BCL-6 / 3q27 chromosome translocation. BCL-2 is an important anti-apoptotic protein, governing the intrinsic apoptotic pathway[8]. It is also highly expressed in 70% of DLBCL patients[9,10]. Overexpression of BCL-2 leads to poor prognosis in patients with DLBCL after first-line treatment[11–14]. Venetoclax (ABT-199), a small-molecule inhibitor selectively targeting BCL-2, has been approved by more than 50 countries as the treatment of adult chronic lymphocytic leukemia (CLL)[15,16]. ABT-199 has shown superior clinical activity in almost all cases of chronic lymphocytic leukemia. In recent years, studies have shown that ABT-199 has unlimited application potential in DLBCL

and can significantly improve the survival rate and clinical symptoms of patients, which is gratifying for patients and researchers. However, despite of the progress of research, it is found that ABT-199 leads to different degrees of drug resistance in DLBCL treatment, which also limits the application of ABT-199 in DLBCL.

Reversing ABT-199 induced drug resistance has become a common challenge for researchers and clinicians. In the clinical treatment of leukemia, the main way to overcome ABT-199 resistance is to combine with other chemotherapeutic drugs such as Azacytidine[17]. Our previous research demonstrated that CS2164 (Chiauranib, targeting tumorigenesis-associated pathways) combined with ABT-199 improved the prognosis of B-cell lymphoma[18]. However, compared with CS2164, Apatinib has a higher antitumor activity in advanced cancers[19]. Apatinib (YN968D1), a small molecule tyrosine kinase receptor inhibitor selectively targeting VEGFR-2[20,21], has been applied to patients with advanced gastric cancer in China[22]. Moreover, Apatinib has been used in phase II / III clinical trials of solid tumors (such as non-small cell lung cancer, breast cancer, and hepatocellular carcinoma)[23–25]. For patients with advanced esophageal squamous cell carcinoma (ESCC) who failed to response to first-line chemotherapy drugs, the median progression-free survival (PFS) was 6.23 months, 2 (16.67%) patients achieved partial remission, and 9 (75.00%) achieved stable disease after they used Apatinib combined with S-1regimen[26]. *In vitro* and phase I clinical studies have found the potential additive or synergistic antitumor effects between anti-PD-1 antibodies and VEGF/VEGFR2 inhibitors[27,28], which prompted us to investigate whether Apatinib combined with ABT-199 can exert a better therapeutic effect in DLBCL.

In this study, we sought to verify the potential synergistic antitumor effect of a regimen combining ABT-199 with Apatinib in DLBCL. Administration of low-dose ABT-199 potentiates the cytotoxicity of Apatinib in various human DLBCL cell lines and primary DLBCL samples, as well as antitumor efficacy in xenograft mouse models. Mechanistically, ABT-199 combined with Apatinib can synergistically kill DLBCL cells by regulating EDN1 and related MAPK/ERK/MEK pathway to alter the balance of pro-apoptotic vs. antiapoptotic BCL-2 proteins without a significant increase in systemic toxicity.

Materials And Methods

Drugs and reagents

ABT-199 and Apatinib were purchased from Selleck Chemicals (Houston, TX, USA). The reagents were prepared as 10 mM stock solution in 100% dissolved in dimethyl sulfoxide (DMSO; Invitrogen, Carlsbad, CA, USA) stored at -20°C, then diluted to the required concentrations according to the manufacturers' instructions.

Cell lines and cell culture

Human DLBCL cell lines MCA, OCI-Ly1, OCI-Ly3, OCI-Ly10, and SU-DHL-4 were purchased from ATCC (Rockefeller, MD, USA) and DLBCL cell lines were grown in RPMI-1640 medium (Gibco, Life Technologies,

NY, USA). OCI-Ly3 cells were cultured in IMDM (Gibco, Life Technologies, NY, USA). Supplemented with 10% fetal bovine serum (HyClone, Thermo Scientific, MA, USA) at 37°C in a humidified CO_2 incubator. Primary DLBCL patients (n=12) at the Department of Hematology, the First Affiliated Hospital, College of Medicine, Zhejiang University (Hangzhou, China). This study was approved by the Ethics Committee of the First Affiliated Hospital of Zhejiang University.

Cell viability assay

The cytotoxic effect of ABT-199 and Apatinib toward DLBCL cells was tested by Cell Counting Kit-8 (CCK-8) assay (Dojindo, Kumamoto, Japan). In brief, cells (2×10^4 cells/well) were seeded in 96-well plates containing 100 μl growth medium and treated with different concentrations of ABT-199 or Apatinib alone or in combination for 12 h or 24 h. CCK-8 reagents (10 μl/well) were added and incubated for an additional 2-4 h at 37 °C, then the absorbance at 450 nm was detected by a microplate reader (ELx800; BioTek Instruments Inc., Winooski, VT, USA). Experiments were implemented in triplicate for each cell line. In the light microscopic experiment, cells were seeded in 24-well plates and treated with different concentrations of ABT-199 or Apatinib alone or in combination for 24 h. The results of cells were performed under a light microscope.

Flow cytometric assay for determining apoptosis, cell cycle, and mitochondrial membrane potential (MMP), and reactive oxygen species (ROS)

To assess apoptosis, DLBCL cells were treated with different concentrations of ABT-199 and Apatinib alone or in combination for 12 and 24 h, according to the manufacturer's instruction. DLBCL cells were harvested and then analyzed by Novocyte (ACEA Bioscience, San Diego, CA, USA) after Annexin V/PI (Thermofisher, USA) staining for 15 min at room temperature in the dark. Primary DLBCL bone marrow or tissue samples were subjected to leukocyte separation. We used the Click-iT EdU Kit (Thermofisher) to test the cell cycle. Loss of the mitochondrial membrane potential (Δψm) was detected using JC-1 Fluorescent Probe Kit (Beyotime Company, Shanghai, China). To evaluate the interaction between ABT-199 and Apatinib, CalcuSyn software was used to calculate the combination index (CI). We used a Reactive Oxygen Species Assay Kit (Beyotime, Shanghai, China) as previously reported to detect the level of cellular ROS, and results were showed as the ratio of the mean fluorescence intensity.

Clonogenic assay

We used colony-forming assay to verify the inhibition effect of ABT-199 and Apatinib alone or in combination, DLBCL cells were treated with different concentrations of agents, and then cells were planted in methylcellulose medium (Methocult H4100, Stem Cell Technologies, Vancouver, BC, Canada) at a density of 500 cells/well for about 14 days. The clone was stained with MTT and counted for tumor-forming capability *in vivo*, and the size of clonogenic was observed under a light microscope.

Western Blot analysis

OCI-Ly1 and MCA cells were lysed at 4°C in lysis buffer and were electrophoresed in 10% SDS-PAGE then transferred to a NC membrane (Millipore, Billerica, MA, USA). The membranes were blocked for 1.5 h with 5% nonfat milk in TBS-T and then probed with primary antibodies (1:1000 in 5% bovine serum albumin in TBS-T) overnight at 4 °C according to the manufacturers, followed by secondary HRP-conjugated antibody (1:20000; Multi Sciences Biotech) and visualized with an ECL detection kit (Biological Industries, Beit HaEmek, Israel). The primary antibodies against EDN1, VEGFR2, p-VEGFR2, ERK, p-ERK, P38, p-P38, MEK, p-MEK, Caspase 3, PARP, BAX, BIM, BCL-2, MCL-1, and β-actin were purchased from Cell Signaling Technology (Danvers, MA, USA).

RNA sequencing

Cells were incubated with ABT-199 with or without Apatinib for 24 h, then total RNA was extracted. RNA sequencing (RNAseq) was then carried out via a biological company (service ID# F20FTSECWLJ3511, BGI, Huada Gene, Wuhan, China). Briefly, the sequencing data was filtered with SOAPnuke (v1.5.2)[29] by (1) Removing reads containing sequencing adapter; (2) Removing reads whose low-quality base ratio (base quality less than or equal to 5) is more than 20%; (3) Removing reads whose unknown base ('N' base) ratio is more than 5%, afterward clean reads were obtained and stored in FASTQ format. The clean reads were mapped to the reference genome using HISAT2[30]. Bowtie2(v2.2.5)[31] was applied to align the clean reads to the reference coding gene set，then the expression level of the gene was calculated by RSEM (v1.2.12) The heatmap was drawn by Pheatmap (v1.0.8) according to the gene expression in different samples. Essentially, differential expression analysis was performed using the DESeq2(v1.4.5)[32] with a Q value ≤ 0.05. To take an insight into the change of phenotype, GO (Gene ontology) (http://www.geneontology.org/) and KEGG (https://www.kegg.jp/) enrichment analysis of annotated different expressed genes was performed
by Phyper (https://en.wikipedia.org/wiki/Hypergeometric_distribution) based on Hypergeometric test. The significant levels of terms and pathways were corrected by Q value with a rigorous threshold (Q value ≤ 0.05) by Bonferroni[33]. Pathway activity network was constructed using Cytoscape[34] for graphical representations of enriched biological pathways with significance ($P < 0.05$), including upregulated and downregulated ones.

In vivo study of Apatinib/ABT-199 efficacy in DLBCL mouse models

The animal study was approved by the First Affiliated Hospital, College of Medicine, Zhejiang University. For model #1, 4~6 week-old female BALB/C nude mice (purchased from Zhejiang University Animal Center) were injected subcutaneously with 2×10^7 OCI-Ly1 cells at the right flank of mice. When the tumor volume reached ~75 mm^3, mice were randomly divided into four groups (n = 5/group), including control, ABT-199, Apatinib, and combination, and then the drugs were given for 2 consecutive weeks with control (vehicle, 0.2% methyl cellulose and 0.1% Tween-80 in PBS), Apatinib (administered by oral gavage at the dose of 100 mg/kg/day), ABT-199 (80 mg/kg/day, oral gavage), or combination of ABT-199 and Apatinib, respectively. During the administration, the mice were monitored daily and their weight was recorded for toxicity. Two weeks after treatment, the tumor size was measured daily by caliper we calculated the

volume (V) of the tumor using the equation: $V = (L \times W^2)/2$, where L and W represent the length and width, respectively. The tumor tissue was subjected to immunohistochemical staining with human CD45 antibody and Western Blot analysis.

For model #2, after the knockdown of the EDN1 gene, MCA and OCI-Ly1 cell line was injected subcutaneously into female BALB/C nude mice. Mice were monitored and weighed daily. After two weeks, subcutaneous tumors were stripped, and maximal diameter (L) and short diameter (W) of the tumor were measured.

Gene overexpression and knockdown

The open-reading frame of human EDN1 cDNA was inserted into the lentiviral transfer vector pLV-EF1a-IRES-EGFP and verified the construction by Sanger sequencing. EDN1 was knocked down by lentiviral transduction using an EDN1-specific shRNA transfer vector targeting residues 2494-PGMLV-SC5 (shEDN1-1) and PGMLV-6395 (shEDN1-2) on RefSeq NM_001955.5. We used 293T to package the lentivirus and harvested it at 48 and 72 h. The target cells were transduced for 2 consecutive days and added 6 μg/mL of polybrene. After 48 hours of transfection, the fresh medium containing puromycin (1 μg/mL) was replaced. Western Blot was used to detect the effect of overexpression and knockout.

Statistical analysis

All experiments were performed in triplicate when indicated, and the value was expressed as the mean ± standard deviation (S.D.). GraphPad Prism 7 software was used for statistical data. The Student's t-test was used for mean comparison between two groups. Multiple-group comparisons were performed using the one-way analysis of variance followed by the Bonferroni post hoc test. To verify the combination effect, we used CalcuSyn v2.0 software for calculating the "combination index" (CI). Synergism (CI < 1), addictive effect (CI = 1), or antagonism (CI > 1)[35]. $P < 0.05$ was considered statistically significant, and different levels were described as $^*P < 0.05$, $^{**}P < 0.01$, and $^{***}P < 0.001$, respectively. All statistical analyses were performed using SPSS 20.0 software (La Jolla, CA).

Results

ABT-199 cooperates with Apatinib to reduce the viability of diverse DLBCL cells

In hematological malignancies, ABT-199 resistance is associated with a variety of gene mutations. On this basis, we enriched the mutated genes by GO. This requires us to use other chemotherapy drugs in combination when treating patients. In addition, compared with the normal group, patients with DLBCL had high expression of BCL-2 **(Fig. 1A, S. 1A)**. To evaluate the potential cooperative effect of ABT-199 and Apatinib we assessed the effect on cell viability. Various DLBCL cell lines were treated with indicated concentrations of ABT-199 and Apatinib, under an electron microscope we found the cells shrinkage, and the fragmentation of membrane blebs **(Fig. 1B, S. 1B)**, after which cell viability was tested using CCK-8 assay. Treatment with ABT-199 and Apatinib alone effectively inhibited cell growth in a dose-dependent

manner. Notably, co-administration of ABT-199 and Apatinib led to markedly enhanced growth inhibition in all of these DLBCL cell lines **(Fig. 1C, 1D, S. 1C, S. 1D, and S. 1E)**. The half-maximal inhibitory concentration (IC50) values **(Table 1)** of ABT-199 and Apatinib were lower at 24 h than at 12 h in all cell lines ($P < 0.001$). Then we examined whether the combination of ABT-199 and Apatinib affects the clonogenicity of DLBCL cells. The size of colonies was observed under an electron microscope and visualization. As shown in **Fig. 1E, 1F, 1G, 1H, S. 2A, S. 2B, S. 2C, and S. 2D** the colony-forming assay revealed that compared with ABT-199 and Apatinib monotherapy groups the combination group could significantly inhibit colony formation in all tested cell lines ($P < 0.001$).

Synergetic lethality of combined ABT-199 and Apatinib in DLBCL cells *in vitro*

To further verify the cytotoxicity effect of ABT-199 and Apatinib when used in combination, we treated DLBCL cells with ABT-199 at various concentrations (1, 2, 4 nM) in the presence or absence of different concentrations of Apatinib (10, 20, 40 μM) for 12 h and 24 h and then the percentage of apoptotic cells was detected by Annexin V/DAPI dual staining **(Fig. 2A)**. The results showed that, even though exposure to different concentrations of ABT-199 and Apatinib single treatment can induce a certain degree of apoptosis, these events were significantly enhanced by combined treatment for 12 h and 24 h **(Fig. 2B, 2C, 2D, 2E, 2F)**. The combination index (CI) calculation shows ABT-199 has a strong synergistic effect with Apatinib at different doses (**Table 2)**.

The combination of ABT-199 and Apatinib altered cell cycle distribution, increased ROS generation, and mitochondrial injury

Subsequently, we analyzed the cell cycle status to further characterize the role of low-dose ABT-199 in enhancing Apatinib mediated cytotoxicity. In all tested DLBCL cell lines, compared with the ABT-199 or Apatinib alone, the percentage of S phase cells in the combined group decreased significantly after 24 h treatment, and the cell cycle was arrested in G0/G1 phase **(Fig. 3A, 3B, 3C, 3D, 3E, and 3F)**. In addition, ABT-199 combined with Apatinib also regulated cycle-related proteins **(Fig. 3L)**. Consistent with the results of apoptosis, ABT-199 and Apatinib also induced loss of mitochondrial membrane potential (MMP), reflected by markedly decreased fluorescence intensity ratio between JC-1 aggregate and monomer **(Fig. 3G, 3H)**. To uncover the potential mechanism of apoptosis induced by these two agents, flow cytometry was used to detect intracellular ROS levels. After being co-treated with ABT-199 and Apatinib for 24 h, a notable increase in ROS generation was observed in OCI-Ly1 and MCA **(Fig. 3I, 3K)**, compared to treatment with each single agent. In addition, our results showed that ABT-199 and Apatinib exerted an anti-proliferative and anti-apoptosis effect in DLBCL cells by inhibiting the MAPK/ERK and pro-survival pathways in OCI-Ly1 and MCA cell lines **(Fig. 3J)**.

The regimen combining ABT-199 and Apatinib impairs tumor-forming capabilities in a xenograft model

To confirm the therapeutic effect of BCL-2 inhibitor combined with Apatinib on DLBCL *in vivo*, we tested the efficacy of ABT-199 plus Apatinib in the BALB/C nude mice (**Fig. 4A)**. The DLBCL cell line OCL-Ly1 was subcutaneously injected for about 7 days, and the treatment was started when the tumor volume

reached to ~75mm^3, mice were randomly divided into the vehicle, ABT-199 (80 mg/kg), Apatinib (100 mg/kg), and the combination of ABT-199 plus Apatinib groups for 14 consecutive days, respectively. Interestingly, compared with the vehicle control as well as each agent, the combined group significantly reduced tumor burden, reflected by decreasing volume and weight of tumor **(Fig. 4B, 4D, and 4E)**. In addition, the weight of mice did not decrease significantly and no other signs of notable toxicity were observed **(Fig. 4C)**. Histological examination showed that the combination treatment inhibited the infiltration of DLBCL cells, while diseased mice treated with ABT-199 or Apatinib alone had more severe DLBCL infiltration **(Fig. 4F)**. Western Blot revealed that the MAPK/ERK pathway was inhibited, which is consistent with the results *in vitro* **(Fig. 4G)**. Together, these findings argue that ABT-199 and Apatinib might interact to cause robust apoptosis and inhibition of DLBCL cells by downregulation MAPK/ERK pathway and anti-apoptotic BCL-2 family proteins as well as upregulation of pro-apoptotic BAX in DLBCL cells.

Combined treatment with ABT-199 and Apatinib ameliorates DLBCL primary patient cells *in vitro* and *in vivo*

The anti-tumor effect of ABT-199 and Apatinib alone or in combination was further verified ex vivo in the primary blasts isolated from 12 DLBCL patients. We summarized the characteristics of the patients in **Table 3**. Following the results obtained from DLBCL cell lines, cotreatment of primary DLBCL blasts with ABT-199 at the concentrations ranging from 0.5 to 16 nmol/L and Apatinib from 5 to 160 μmol/L caused remarkable inhibited cells proliferation when compared with each agent alone **(Fig. 5A, 5B, 5C, 5D, 5E, 5F, 5G, 5H, 5I, 5J, and 5K)**. We detected the apoptosis of primary DLBCL blasts and found that ABT-199 and Apatinib could significantly induce apoptosis, which was consistent with the results in cells lines **(Fig. 5L)**. Similarly, Western Blot results showed that MAPK/ERK pathway and anti-apoptotic BCL-2, MCL-1 were significantly inhibited **(Fig. 5M)**. Together, these results indicate that the combination of ABT-199 with Apatinib might be a preferable choice to targeted DLBCL blasts.

Co-treatment with ABT-199 and Apatinib alters genome-wide gene expression in DLBCL cells

To screen for the molecular target of co-treatment with ABT-199 and Apatinib, we performed RNA sequencing in the samples of DLBCL cells treated with ABT-199 and/or Apatinib. We found that 189 genes were differentially expressed after co-treatment ABT-199 and Apatinib compared with that in the single-treated samples **(S. Table1)**. GO analysis indicated that multicellular organismal development was upregulated, while terms including oxidation-reduction process, inflammatory response, oxygen transport, and cell killing were downregulated **(Fig. 6A, 6B)**. Pathway analysis revealed that Natural killer cell-mediated cytotoxicity, VEGF signaling pathway, and ECM-receptor interaction were significantly elevated. Meanwhile, the MAPK signaling pathway and ErbB signaling pathway were downregulated **(Fig. 6C, D)**. Five key genes including HGF, EDNZ, SPP1, HMOX1, CCL5, ADM were significantly enriched according to the pathway activity network **(Fig. 6E, 6F)**. Different K-cores were used to identify core regulatory genes involved in DLBCL treatment. As shown in **Fig. S. 3C**, we found that EDN1 was most possibly related to DLBCL development, which achieved a high ranking among the top 5 genes in terms of different K-cores

after excluding genes with low abundance and matrix-related genes. Thus, we hypothesized that co-treatment exhibited its DLBCL attenuation effect by activating EDN1. GO analysis was used to analysis differentially expressed genes treated with ABT-199 and/or Apatinib for 3 days (all DEGs) and the percentage of GO term in the combination treatment group is shown in the pie chart from the DLBCL cells transcriptome (all DEGs) **(Fig. S. 3A, S. 3B)**.

Endothelin-1(EDN1) gene plays an important role in apoptosis induced by ABT-199 and Apatinib

EDN1 is considered to be the most effective vasoconstrictor in the human cardiovascular system and plays a vital role in the development of tumors. In the previous study, we found the EDN1 gene through RNAseq assay, and it was also an anti- apoptotic protein that affects the overall survival and disease-free survival **(Fig. 7A, 7B)**. Therefore, we verified its role in DLBCL by overexpression and knockdown of the EDN1 gene. Western Blot and flow cytometry showed the effect of overexpression of EDN1 gene in OCI-Ly1 and MCA cell lines **(Fig. 7C, 7D, 7F, 7 G and S. 2E, S. 2F)**. Then we knocked out the EDN1 gene, and Western Blot was used to verify the knockout effect of EDN1 **(Fig. 7H, 7I)**. Compared with the scramble, the expression of the EDN1 significantly decreased. The cell counts and the colony-forming also obviously decreased after shRNA interference **(Fig. 7J, 7K, 7E, 7N, 7O, and S. 2G)**. The flow cytometry results also showed that the proportion of apoptosis of OCI-Ly1 and MCA cell lines after interference was remarkably increased as shown in **Fig. 7L, 7M**.

shRNA interference of EDN1 gene inhibits tumor burden in mice

To further explore the effect of EDN1 knockout *in vivo*, we selected BALB/C nude model mice and injected EDN1 knockout OCI-Ly1 and MCA cell lines into mice respectively. According to the results of cell lines, EDN1 gene knockout can effectively inhibit the growth of tumor cells and reduce tumor load, reflected by decreased volume and weight of tumor masses, compared to vehicle control and each agent **(Fig. 8A, 8D, 8E, 8F, 8I, 8J)**. In addition, there was no significant difference in body weight between NC group and shEDN1 group **(Fig. 8B, 8G)**. Histological examination found that the shEDN1 group remarkably inhibited the infiltration of DLBCL cells **(Fig. 8C, 8H)**. After the mice were killed we ground the stripped tumor and extracted proteins, the results are consistent with those of cell lines. ABT-199 and Apatinib inhibited the MAPK/ERK and pro-survival pathways in the xenograft model **(Fig. 8K, 8L)**. Thus, a mechanism involving ABT-199 and Apatinib apoptotic network is presented in hematologic malignancies **(Fig. 8M)**.

Discussion

Although the first-line treatment R-CHOP (rituximab, cyclophosphamide, doxorubicin, vincristine, and prednisolone) and other conventional therapies combining multiple chemotherapeutic drugs have greatly improved the survival of many patients with DLBCL, this disease remains incurable[36–39]. Therefore, new agents and drug combinations with less systemic toxicity are urgently needed. ABT-199, a selective targeting inhibitor of BCL-2, has emerged as a promising treatment strategy for some B-cell malignancies such as CLL (chronic lymphocytic leukemia) and MCL (mantle cell lymphoma). However, the therapeutic

effect of ABT-199 alone in DLBCL is limited[40]. In this study, we found a regimen combining BCL-2 inhibitor ABT-199 with tyrosine kinase inhibitor Apatinib exerting superb anti-tumor activity against DLBCL cells and patients, and this combination regimen showed superior effects on cells from different DLBCL subtypes carrying diverse genetic alterations in the *in vitro, ex vivo*. In addition, we observed that ABT-199 combined with Apatinib was highly active in a BALB/C nude mouse model indicating the promising activity of this regimen for the treatment of high-risk DLBCL patients with poor prognosis. Our previous research confirmed that CS2164 combined with ABT-199 improved the prognosis of B-cell lymphoma. Compared with CS2164 and ABT-199, Apatinib and ABT-199 have a higher antitumor activity of advanced cancers. In the treatment of B-cell lymphoma, the IC50 value of ABT-199 combined with Apatinib is lower than that with CS2164. Thus, the regimen combining ABT-199 and Apatinib may represent an effective regimen to treat DLBCL.

Angiogenesis plays an important role in the development and metastasis of tumors. It is also an essential part of the growth of tumor cells[41–43]. Tumor angiogenesis is related to the activation of VEGF by binding to its specific receptor (VEGFR). Notably, the overexpression of VEGF and VEGFR correlates with the metastasis and microvessel density of many kinds of malignancies, so the prognosis is poor[44]. Therefore, VEGFR is a promising target for tumor therapy. Researchers reported that VEGF was also shown to enhance endothelial cell survival by upregulating BCL-2 expression through a pathway mediated by VEGFR2 and phosphatidylinositol 3-kinase/Akt signaling[45–47]. In this paper, we verified that exposure to Apatinib resulted in marked p-VEGFR2 and BCL-2 downregulation, and BAX upregulation. This reveals that the expression of VEGFR2 will cause the expression of the anti-apoptotic protein BCL-2. Therefore, simultaneous inhibition of VEGFR2 and BCL-2 can effectively inhibit the growth of DLBCL cells. Moreover, our RNA sequencing results showed that ABT-199 combined with Apatinib regulated endothelin 1 (EDN1) gene, and EDN1 exerted anti-proliferative effects by inhibiting the MAPK/ERK and pro-survival pathways as shown in Fig. 6 and Fig. 7. Thus, these findings support the notion that EDN1 may play a key role in the combination of ABT-199/Apatinib. They also propose a potential mechanism for the interaction between ABT-199 and Apatinib, in which while ABT-199 inhibits BCL-2 expression, accompanied by Apatinib decreases p-VEGFR2 expression.

Aberrant activation of the endothelin 1 (EDN1) axis is now generally considered a common mechanism underlying the progression of various solid tumors, including ovarian, prostate, colon, breast, bladder, and lung cancers, which is an important adverse factor affecting the prognosis[48–50]. Besides, the function of the EDN1 gene is related to the activation of the MAPK pathway[49]. In this study, we found that co-treatment with ABT-199 and Apatinib resulted in marked EDN1 inhibition in DLBCL cells. On the contrary, ABT-199 or Apatinib alone could not inhibit the expression of EDN1. These observations proved that the EDN1 gene may play a crucial role in regulating the synergistic killing effect of DLBCL by ABT-199 and Apatinib (Fig. 6 and Fig. 7).

The bulk of research on ABT-199 and Apatinib alone in DLBCL has been widely published, especially ABT-199, but the research combining ABT-199 and Apatinib for the treatment of DLBCL has not been studied

so far. Particularly those hard-to-treat subtypes. In this context, our study found that ABT-199/Apatinib was also effective on OCI-Ly1, OCI-Ly3, and OCI-Ly10 cell lines from activated B-cell–like (ABC) which expression of BCL-6, CD10, and MUM1[40], as well as primary DLBCL blasts from patients. In addition, the efficacy of this regimen was further replicated in BALB/C nude mouse model. Moreover, the weight change and mental state of experimental mice showed that the toxicity and side effects of this regimen were small. Taken together, our results strongly suggest that the combination of ABT-199 and Apatinib regimen might represent an effective therapy for the treatment of DLBCL patients, and future studies are warranted to include more PDX models.

Strikingly, our regimen is effective not only for patients with primary DLBCL but also for refractory/relapsed patients, implying that the combination regimen could rapidly and potently diminish tumor burden in DLBCL patients. In addition, we also found that the combined regimen did no effect on peripheral WBC of healthy people, indicating that the regimen had less toxic and side effects on DLBCL patients. It might also provide a theoretical basis for the clinical application of the combined regimen, although it needs to be further examined.

In summary, our study provides strong preclinical evidence to support that the regimen combining ABT-199 and Apatinib is highly effective towards DLBCL with diverse cytogenetic and genetic aberrations, including refractory/relapsed patients. Therefore, the novel combination regimen warrants further clinical investigation in the treatment of DLBCL patients, especially those with multiple gene mutations.

Declarations

Author contributions

Y. F. Shi and J Ye performed the experiments and analysis of data. H. F. Shen, R. Wan and Y Xu collected primary DLBCL samples and interpret data and wrote the manuscript. X. J. Ye, J. Jin and W. Z. Xie contributed to study design, data analysis, and interpretation and manuscript revision.

Funding

This work was supported in part by the Research Plan of the National Natural Science Foundation of China (No.81372256).

Conflicts of interest

The authors declare that they have no potential conflicts of interest.

References

1. Kuo, H. P. *et al.* Combination of Ibrutinib and ABT-199 in Diffuse Large B-Cell Lymphoma and Follicular Lymphoma. *Mol Cancer Ther* **16**, 1246-1256, doi:10.1158/1535-7163.MCT-16-0555 (2017).

2. Sasi, B. K. *et al.* Inhibition of SYK or BTK augments venetoclax sensitivity in SHP1-negative/BCL-2-positive diffuse large B-cell lymphoma. *Leukemia* **33**, 2416-2428, doi:10.1038/s41375-019-0442-8 (2019).
3. Dunleavy, K., Erdmann, T. & Lenz, G. Targeting the B-cell receptor pathway in diffuse large B-cell lymphoma. *Cancer Treat Rev* **65**, 41-46, doi:10.1016/j.ctrv.2018.01.002 (2018).
4. Lavacchi, D. *et al.* Pharmacogenetics in diffuse large B-cell lymphoma treated with R-CHOP: Still an unmet challenge. *Pharmacol Ther*, 107924, doi:10.1016/j.pharmthera.2021.107924 (2021).
5. Collinge, B. *et al.* The impact of MYC and BCL2 structural variants in tumors of DLBCL morphology and mechanisms of false-negative MYC IHC. *Blood* **137**, 2196-2208, doi:10.1182/blood.2020007193 (2021).
6. Correction: Targeting of BCL2 Family Proteins with ABT-199 and Homoharringtonine Reveals BCL2- and MCL1-Dependent Subgroups of Diffuse Large B-Cell Lymphoma. *Clin Cancer Res* **22**, 3984, doi:10.1158/1078-0432.CCR-16-1315 (2016).
7. Lenz, G. *et al.* Stromal gene signatures in large-B-cell lymphomas. *N Engl J Med* **359**, 2313-2323, doi:10.1056/NEJMoa0802885 (2008).
8. Hata, A. N., Engelman, J. A. & Faber, A. C. The BCL2 Family: Key Mediators of the Apoptotic Response to Targeted Anticancer Therapeutics. *Cancer Discov* **5**, 475-487, doi:10.1158/2159-8290.CD-15-0011 (2015).
9. Valera, A. *et al.* MYC protein expression and genetic alterations have prognostic impact in patients with diffuse large B-cell lymphoma treated with immunochemotherapy. *Haematologica* **98**, 1554-1562, doi:10.3324/haematol.2013.086173 (2013).
10. Ennishi, D. *et al.* Genetic profiling of MYC and BCL2 in diffuse large B-cell lymphoma determines cell-of-origin-specific clinical impact. *Blood* **129**, 2760-2770, doi:10.1182/blood-2016-11-747022 (2017).
11. Hu, S. *et al.* MYC/BCL2 protein coexpression contributes to the inferior survival of activated B-cell subtype of diffuse large B-cell lymphoma and demonstrates high-risk gene expression signatures: a report from The International DLBCL Rituximab-CHOP Consortium Program. *Blood* **121**, 4021-4031; quiz 4250, doi:10.1182/blood-2012-10-460063 (2013).
12. Huang, S. *et al.* Prognostic impact of diffuse large B-cell lymphoma with extra copies of MYC, BCL2 and/or BCL6: comparison with double/triple hit lymphoma and double expressor lymphoma. *Diagn Pathol* **14**, 81, doi:10.1186/s13000-019-0856-7 (2019).
13. Kadia, T. M. *et al.* Venetoclax plus intensive chemotherapy with cladribine, idarubicin, and cytarabine in patients with newly diagnosed acute myeloid leukaemia or high-risk myelodysplastic syndrome: a cohort from a single-centre, single-arm, phase 2 trial. *Lancet Haematol* **8**, e552-e561, doi:10.1016/S2352-3026(21)00192-7 (2021).
14. Crump M, Neelapu SS, Farooq U, et al. Outcomes in refractory diffuse large B-cell lymphoma: results from the international SCHOLAR-1 study. Blood. 2017;130(16):1800-1808. *Blood* **131**, 587-588, doi:10.1182/blood-2017-11-817775 (2018).

15. Seymour, J. F. *et al.* Venetoclax-Rituximab in Relapsed or Refractory Chronic Lymphocytic Leukemia. *N Engl J Med* **378**, 1107-1120, doi:10.1056/NEJMoa1713976 (2018).
16. Davis, J. E. *et al.* Immune recovery in patients with mantle cell lymphoma receiving long-term ibrutinib and venetoclax combination therapy. *Blood Adv* **4**, 4849-4859, doi:10.1182/bloodadvances.2020002810 (2020).
17. Zavras, P. D., Shastri, A., Goldfinger, M., Verma, A. K. & Saunthararajah, Y. Clinical trials assessing hypomethylating agents combined with other therapies: causes for failure and potential solutions. *Clin Cancer Res*, doi:10.1158/1078-0432.CCR-21-2139 (2021).
18. Yuan, D. *et al.* CS2164 and Venetoclax Show Synergistic Antitumoral Activities in High Grade B-Cell Lymphomas With MYC and BCL2 Rearrangements. *Front Oncol* **11**, 618908, doi:10.3389/fonc.2021.618908 (2021).
19. Deng, M. *et al.* Apatinib exhibits anti-leukemia activity in preclinical models of acute lymphoblastic leukemia. *J Transl Med* **16**, 47, doi:10.1186/s12967-018-1421-y (2018).
20. Tian, S. *et al.* YN968D1 is a novel and selective inhibitor of vascular endothelial growth factor receptor-2 tyrosine kinase with potent activity in vitro and in vivo. *Cancer Sci* **102**, 1374-1380, doi:10.1111/j.1349-7006.2011.01939.x (2011).
21. Li, J. *et al.* Randomized, Double-Blind, Placebo-Controlled Phase III Trial of Apatinib in Patients With Chemotherapy-Refractory Advanced or Metastatic Adenocarcinoma of the Stomach or Gastroesophageal Junction. *J Clin Oncol* **34**, 1448-1454, doi:10.1200/JCO.2015.63.5995 (2016).
22. Li, J. *et al.* Apatinib for chemotherapy-refractory advanced metastatic gastric cancer: results from a randomized, placebo-controlled, parallel-arm, phase II trial. *J Clin Oncol* **31**, 3219-3225, doi:10.1200/JCO.2013.48.8585 (2013).
23. Zhang, H. Apatinib for molecular targeted therapy in tumor. *Drug Des Devel Ther* **9**, 6075-6081, doi:10.2147/DDDT.S97235 (2015).
24. Zhao, H. *et al.* Apatinib Plus Gefitinib as First-Line Treatment in Advanced EGFR-Mutant NSCLC: The Phase III ACTIVE Study (CTONG1706). *J Thorac Oncol* **16**, 1533-1546, doi:10.1016/j.jtho.2021.05.006 (2021).
25. Li, X., He, Y., Hou, J., Yang, G. & Zhou, S. A Time-Programmed Release of Dual Drugs from an Implantable Trilayer Structured Fiber Device for Synergistic Treatment of Breast Cancer. *Small* **16**, e1902262, doi:10.1002/smll.201902262 (2020).
26. Zhao, J. *et al.* Clinical efficacy and safety of apatinib combined with S-1 in advanced esophageal squamous cell carcinoma. *Invest New Drugs* **38**, 500-506, doi:10.1007/s10637-019-00866-5 (2020).
27. Xu, J. *et al.* Anti-PD-1 Antibody SHR-1210 Combined with Apatinib for Advanced Hepatocellular Carcinoma, Gastric, or Esophagogastric Junction Cancer: An Open-label, Dose Escalation and Expansion Study. *Clin Cancer Res* **25**, 515-523, doi:10.1158/1078-0432.CCR-18-2484 (2019).
28. Yasuda, S. *et al.* Simultaneous blockade of programmed death 1 and vascular endothelial growth factor receptor 2 (VEGFR2) induces synergistic anti-tumour effect in vivo. *Clin Exp Immunol* **172**, 500-506, doi:10.1111/cei.12069 (2013).

29. Li, R., Li, Y., Kristiansen, K. & Wang, J. SOAP: short oligonucleotide alignment program. *Bioinformatics* **24**, 713-714, doi:10.1093/bioinformatics/btn025 (2008).
30. Kim, D., Langmead, B. & Salzberg, S. L. HISAT: a fast spliced aligner with low memory requirements. *Nat Methods* **12**, 357-360, doi:10.1038/nmeth.3317 (2015).
31. Langmead, B. & Salzberg, S. L. Fast gapped-read alignment with Bowtie 2. *Nat Methods* **9**, 357-359, doi:10.1038/nmeth.1923 (2012).
32. Love, M. I., Huber, W. & Anders, S. Moderated estimation of fold change and dispersion for RNA-seq data with DESeq2. *Genome Biol* **15**, 550, doi:10.1186/s13059-014-0550-8 (2014).
33. Lesack, K. & Naugler, C. An open-source software program for performing Bonferroni and related corrections for multiple comparisons. *J Pathol Inform* **2**, 52, doi:10.4103/2153-3539.91130 (2011).
34. Shannon, P. *et al.* Cytoscape: a software environment for integrated models of biomolecular interaction networks. *Genome Res* **13**, 2498-2504, doi:10.1101/gr.1239303 (2003).
35. Chou, T. C. & Talalay, P. Quantitative analysis of dose-effect relationships: the combined effects of multiple drugs or enzyme inhibitors. *Adv Enzyme Regul* **22**, 27-55, doi:10.1016/0065-2571(84)90007-4 (1984).
36. Pfreundschuh, M. *et al.* CHOP-like chemotherapy plus rituximab versus CHOP-like chemotherapy alone in young patients with good-prognosis diffuse large-B-cell lymphoma: a randomised controlled trial by the MabThera International Trial (MInT) Group. *Lancet Oncol* **7**, 379-391, doi:10.1016/S1470-2045(06)70664-7 (2006).
37. Zoellner, A. K. *et al.* Long-term survival of patients with mantle cell lymphoma after autologous haematopoietic stem-cell transplantation in first remission: a post-hoc analysis of an open-label, multicentre, randomised, phase 3 trial. *Lancet Haematol* **8**, e648-e657, doi:10.1016/S2352-3026(21)00195-2 (2021).
38. Painschab, M. S. *et al.* Comparison of best supportive care, CHOP, or R-CHOP for treatment of diffuse large B-cell lymphoma in Malawi: a cost-effectiveness analysis. *Lancet Glob Health* **9**, e1305-e1313, doi:10.1016/S2214-109X(21)00261-8 (2021).
39. Seymour, E. K. *et al.* Selinexor in Combination with R-CHOP for Frontline Treatment of Non-Hodgkin Lymphoma: Results of a Phase I Study. *Clin Cancer Res* **27**, 3307-3316, doi:10.1158/1078-0432.CCR-20-4929 (2021).
40. Klanova, M. *et al.* Targeting of BCL2 Family Proteins with ABT-199 and Homoharringtonine Reveals BCL2- and MCL1-Dependent Subgroups of Diffuse Large B-Cell Lymphoma. *Clin Cancer Res* **22**, 1138-1149, doi:10.1158/1078-0432.CCR-15-1191 (2016).
41. Longo, R. & Gasparini, G. Challenges for patient selection with VEGF inhibitors. *Cancer Chemother Pharmacol* **60**, 151-170, doi:10.1007/s00280-006-0403-6 (2007).
42. Sullivan, L. A. & Brekken, R. A. The VEGF family in cancer and antibody-based strategies for their inhibition. *MAbs* **2**, 165-175, doi:10.4161/mabs.2.2.11360 (2010).
43. Hanahan, D. & Weinberg, R. A. Hallmarks of cancer: the next generation. *Cell* **144**, 646-674, doi:10.1016/j.cell.2011.02.013 (2011).

44. Banerjee, S., Dowsett, M., Ashworth, A. & Martin, L. A. Mechanisms of disease: angiogenesis and the management of breast cancer. *Nat Clin Pract Oncol* **4**, 536-550, doi:10.1038/ncponc0905 (2007).
45. Gerber, H. P. *et al.* Vascular endothelial growth factor regulates endothelial cell survival through the phosphatidylinositol 3'-kinase/Akt signal transduction pathway. Requirement for Flk-1/KDR activation. *J Biol Chem* **273**, 30336-30343, doi:10.1074/jbc.273.46.30336 (1998).
46. Nor, J. E., Christensen, J., Mooney, D. J. & Polverini, P. J. Vascular endothelial growth factor (VEGF)-mediated angiogenesis is associated with enhanced endothelial cell survival and induction of Bcl-2 expression. *Am J Pathol* **154**, 375-384, doi:10.1016/S0002-9440(10)65284-4 (1999).
47. Kaneko, T. *et al.* Bcl-2 orchestrates a cross-talk between endothelial and tumor cells that promotes tumor growth. *Cancer Res* **67**, 9685-9693, doi:10.1158/0008-5472.CAN-07-1497 (2007).
48. Maguire, J. J. & Davenport, A. P. Endothelin@25 - new agonists, antagonists, inhibitors and emerging research frontiers: IUPHAR Review 12. *Br J Pharmacol* **171**, 5555-5572, doi:10.1111/bph.12874 (2014).
49. Rosano, L., Spinella, F. & Bagnato, A. Endothelin 1 in cancer: biological implications and therapeutic opportunities. *Nat Rev Cancer* **13**, 637-651, doi:10.1038/nrc3546 (2013).
50. Hwang, C. Y. *et al.* Systems analysis identifies endothelin 1 axis blockade for enhancing the anti-tumor effect of multikinase inhibitor. *Cancer Gene Ther*, doi:10.1038/s41417-021-00373-x (2021).

Tables

Table 1 IC50 values of ABT-199 and Apatinib as single agent in DLBCL cells

DLBCL Cell Lines	IC50 at 12h		IC50 at 24h	
	ABT-199 (nM)	Apatinib (μM)	ABT-199 (nM)	Apatinib (μM)
MCA	11.0±1.23	4.6±2.04	4.90±1.61	2.80±0.33
OCI-Ly1	171±1.46	16.2±0.81	31.3±1.82	2.04±1.10
OCI-Ly3	215±1.72	36.1±0.91	54.2±1.33	15.2±0.77
OCI-Ly10	64.1±0.52	23.1±3.40	8.25±1.74	5.92±1.15
SU-DHL-4	26.1±1.33	7.20±2.11	13.3±0.42	5.41±0.53

Table 2 The effect of synergistic inhibition in DLBCL cell lines

DLBCL Cell Lines	Combination Index at 12h			Combination Index at 24h		
	ED50	ED75	ED90	ED50	ED75	ED90
MCA	0.02332	0.01065	0.00494	0.19161	0.04673	0.01201
OCI-Ly1	0.11521	0.04058	0.01439	0.15799	0.05508	0.01937
OCI-Ly3	0.05283	0.01781	0.00632	0.03605	0.00444	0.00058
OCI-Ly10	0.11342	0.03869	0.01332	0.10958	0.03948	0.01446
SU-DHL-4	0.00721	0.00164	0.00086	0.02949	0.00794	0.00216

Table 3 Characteristic of primary DLBCL patients

Patients	Diagnose	Gender	Age (yr)	Karyo-type
DLBCL#1	De novo	F	60	46, XX
DLBCL#2	De novo	M	79	46, XY
DLBCL#3	De novo	M	66	46, XY
DLBCL#4	Refractory	M	83	46, XY
DLBCL#5	De novo	M	67	46, XY
DLBCL#6	De novo	M	80	46, XY
DLBCL#7	De novo	M	71	46, XY
DLBCL#8	Refractory	F	65	46, XX
DLBCL#9	De novo	F	60	46, XX
DLBCL#10	Refractory	F	76	46, XX
DLBCL#11	Refractory	F	66	46, XX
DLBCL#12	De novo	M	87	46, XY

Figures

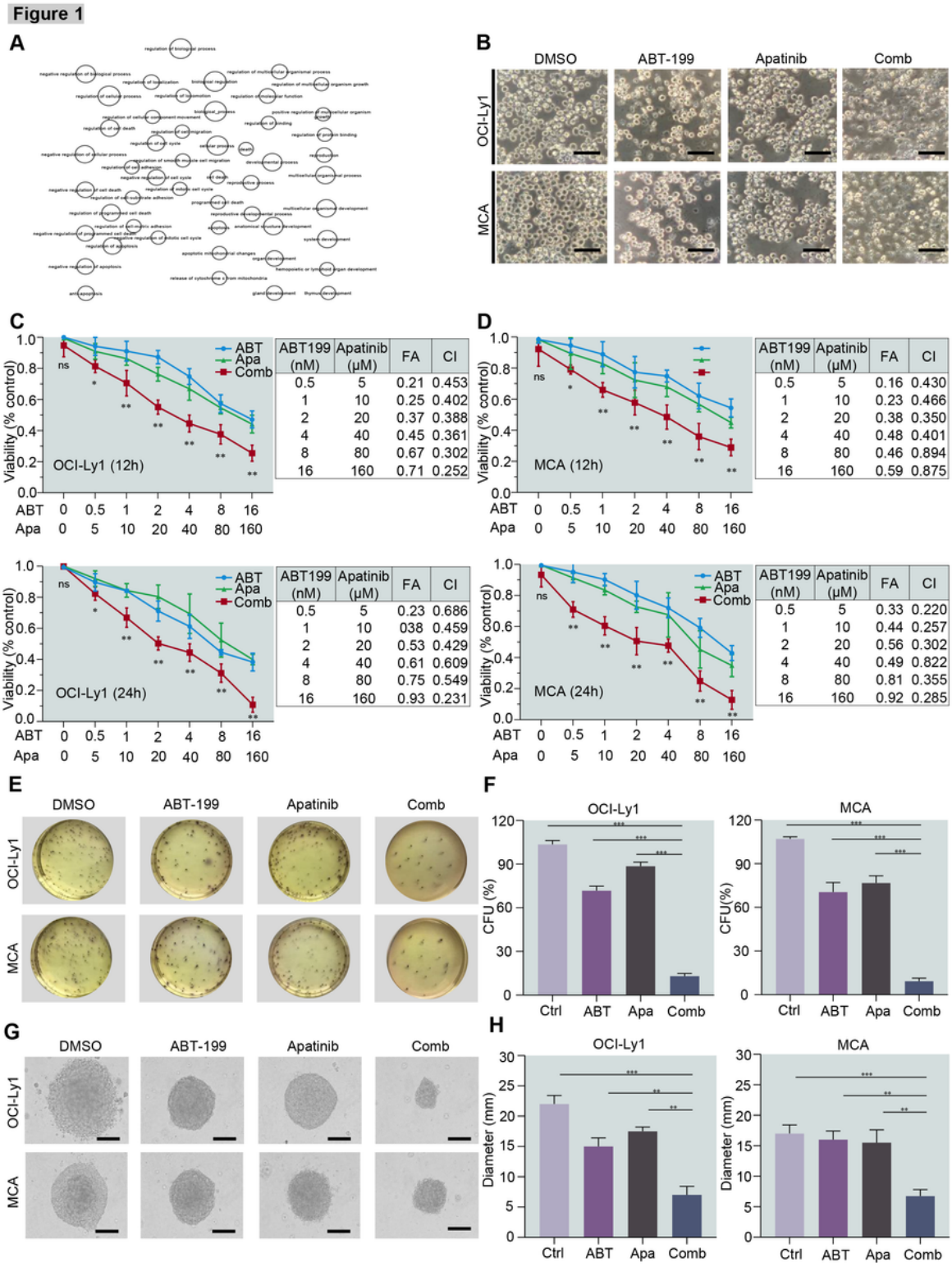

Figure 1

The BCL-2 inhibitor ABT-199 synergistically interacts with the VEGFR2 inhibitor Apatinib to inhibit cell viability in DLBCL cells. (A) ABT-199 resistance is associated with a variety of gene mutations. On this basis, we enriched the mutated genes by GO. (B) Changes in morphology in OCI-Ly1 and MCA cells were incubated with ABT-199 and Apatinib alone or combination treatment for 24 h and visualized using an inverted microscope. Scale bar: 20 μm. (C, D) The inhibition rate of cell viability was measured at 12 h

and 24 h in OCI-Ly1 and MCA cell lines using the CCK-8. (E, F) OCI-Ly1 and MCA cells were treated with ABT-199 (2 nM and Apatinib 20 μM for 24 h, after which the clonogenicity assay was performed to determine the percentage of CFU (left, representative images; right, bar graphs). Values indicate mean ± SD for at least three independent experiments performed in triplicate (*P < 0.05, **P < 0.01, and ***P < 0.001). (G, H) Inverted microscope observed the CFU size and measured its diameter (left, representative images; right, bar graphs).

Figure 2

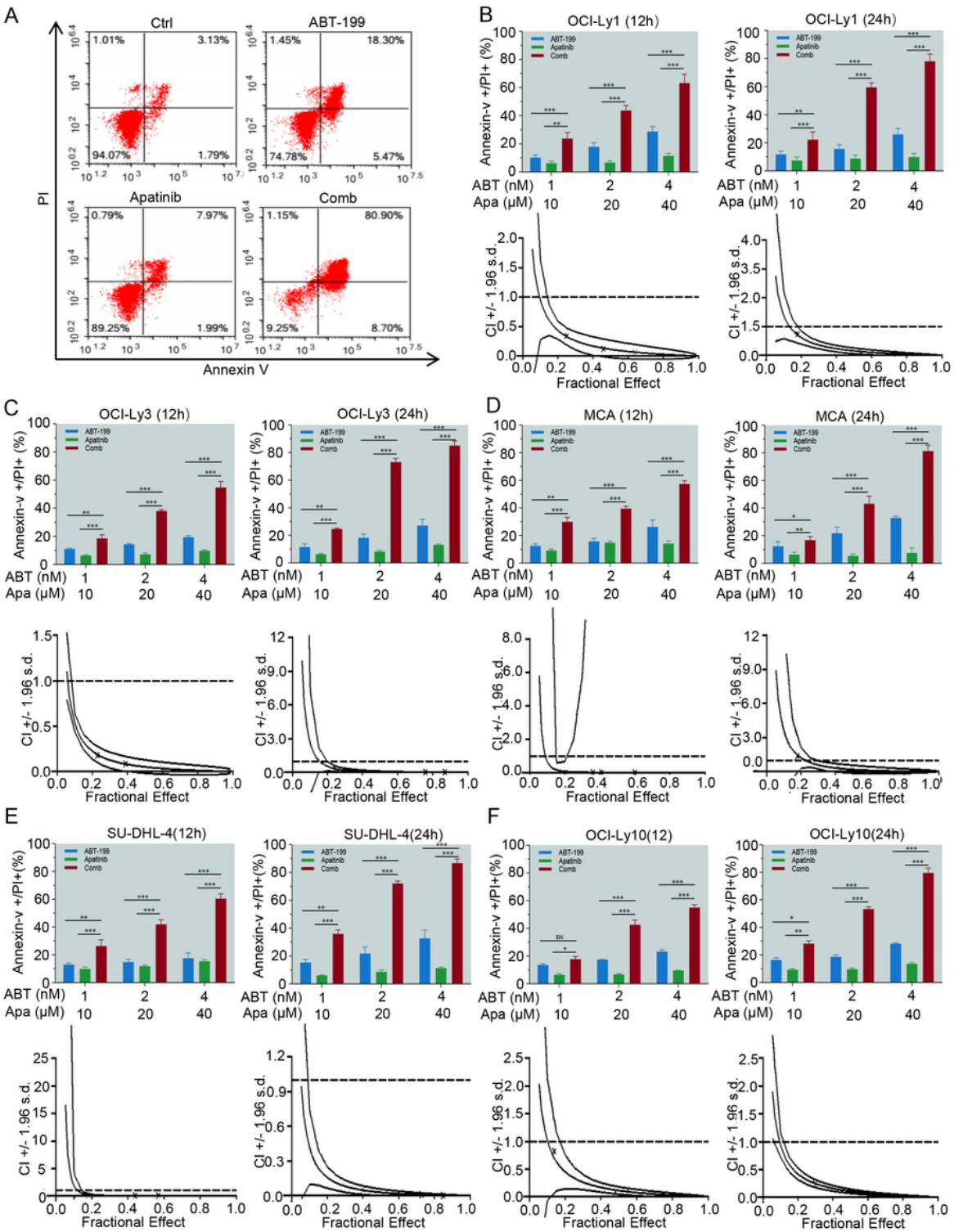

Figure 2

Combination of ABT-199 and Apatinib induces apoptosis in DLBCL cells. (A, B, C, D, E, F) Cells were treated with the indicated concentrations of ABT-199 ± Apatinib for 12 and 24 h, after which the percentage of Annexin-V+ apoptotic cells were determined by flow cytometry after Annexin-V and PI double staining. The combination index (CI) was calculated based on apoptosis using the CalcuSyn software to evaluate the interaction between ABT-199 and Apatinib in DLBCL cell lines (CI < 1.0= 1.0, and >1.0, indicating synergistic, additive, and antagonistic effect, respectively). The apoptotic results and CI index of other cell lines were shown in Supplemental.

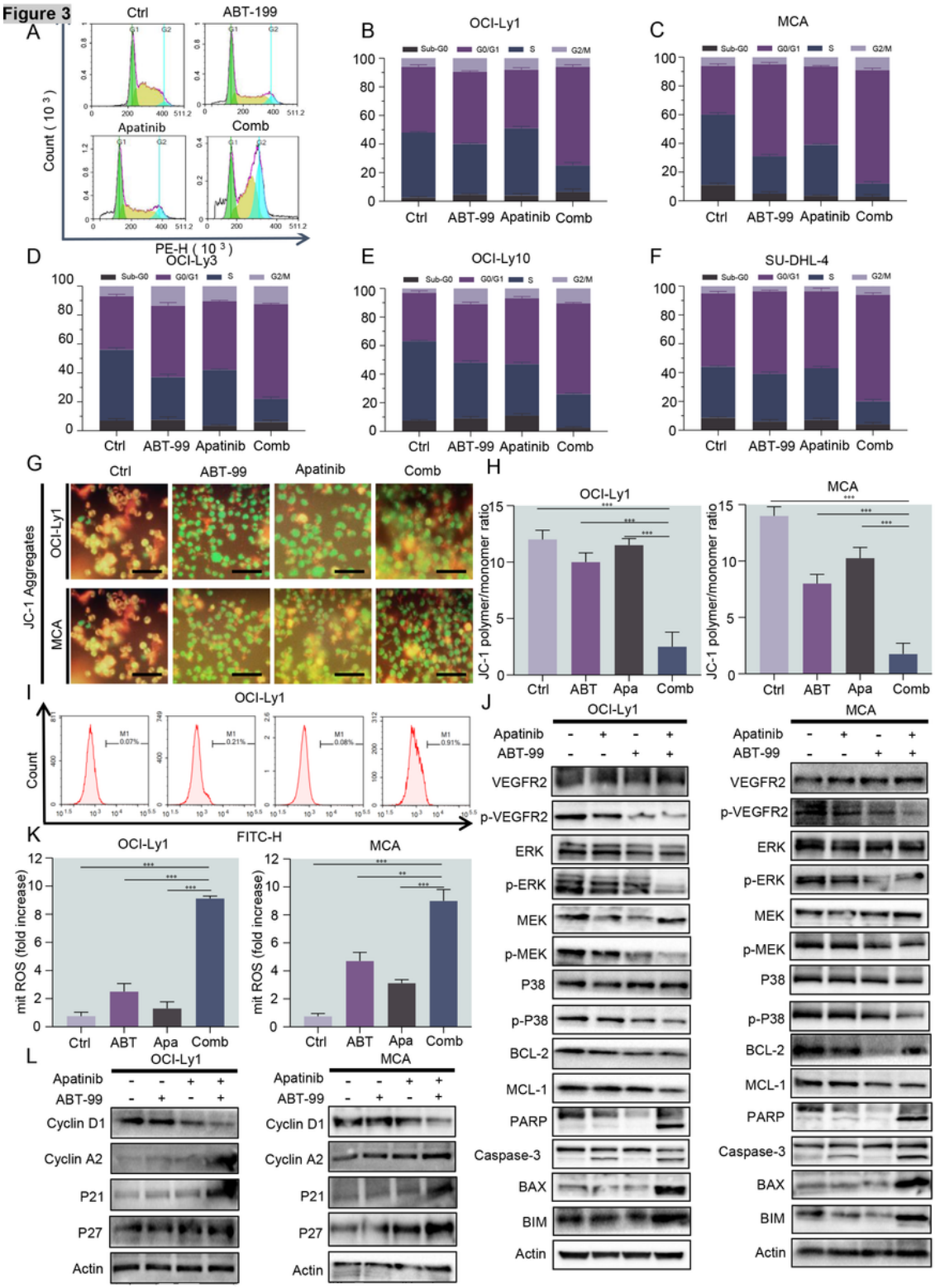

Figure 3

ABT-199 and Apatinib exert the anti-tumor activity towards various diffuse large B-cell lymphoma (DLBCL). (A, B, C, D, E, F) Cell cycle distribution was assessed at 24 h by flow cytometry (black, dark purple, black purple, and lavender present the statistical significance of Sub-G0, G0/G1, S, G2/M between DMSO and Combo group, respectively). (G, H) OCI-Ly1 and MCA cells with loss of mitochondrial membrane potential. (I, K) Meanwhile, intracellular ROS levels were measured by flow cytometry using the Reactive Oxygen Species Assay Kit. Values indicating mean ± SEM for at least three independent experiments performed in triplicate (***P < 0.001). (L) Cell lysates after treatment with ABT-199 and Apatinib alone or combination were collected, and levels of cell cycle-related proteins P21, P27, CyclinA2 and CyclinD1 were determined by Western Blotting with the respective antibodies. (J) OCI-Ly1 and MCA cells were exposed to the indicated concentrations of ABT-199 ± Apatinib for 24 h, after which Western Blot analysis was showed to monitor expression of p-VEGFR2, MAPK pathway associated proteins, antiapoptotic proteins BCL-2 and MCL-1, as well as cleavage of caspase 3 and PARP.

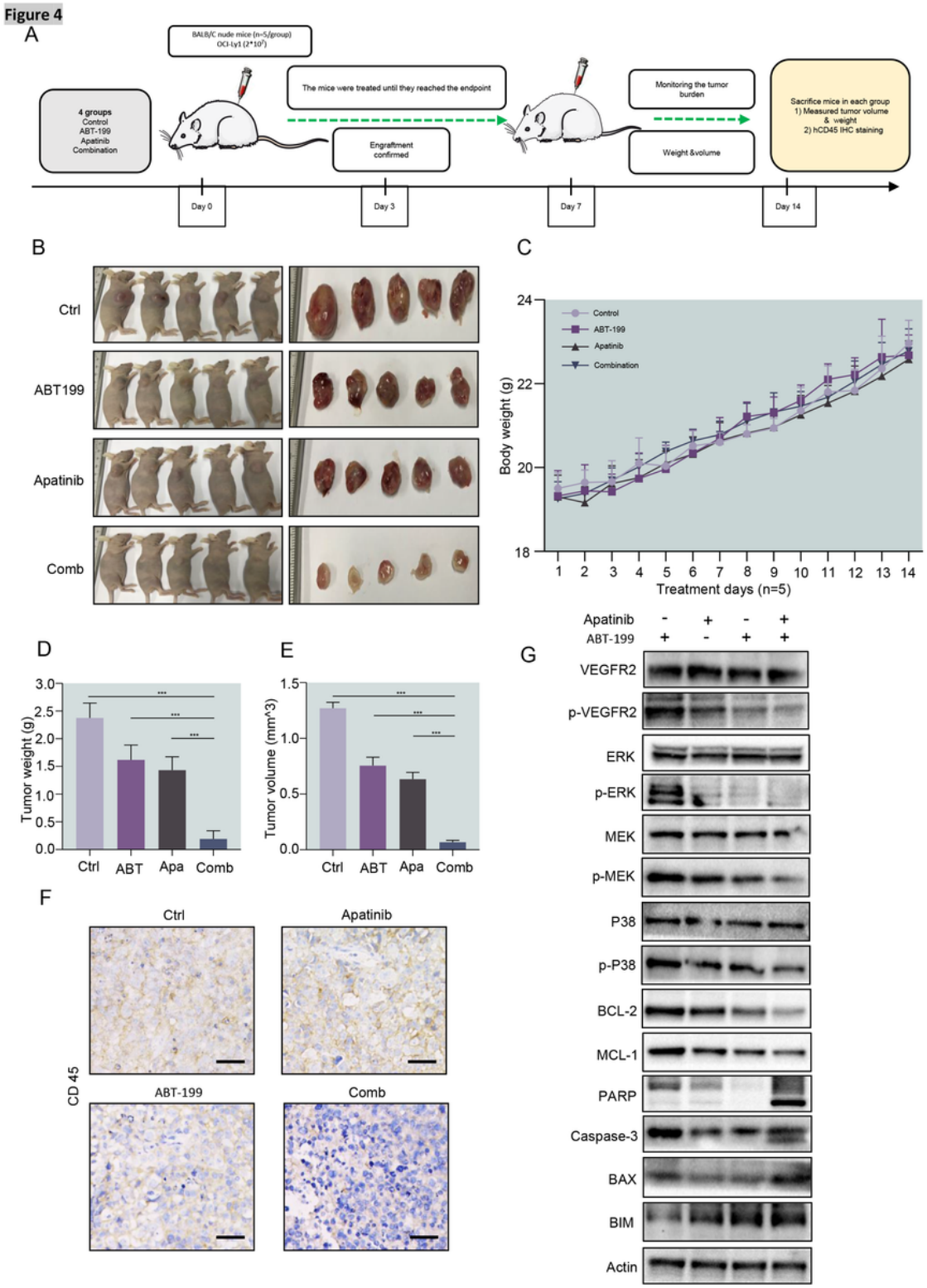

Figure 4

BALB/C nude mice were injected subcutaneously with 2×107 OCI-Ly1 cells at the right flank. Once the tumor volume reached to ~75mm3, mice were randomly divided into four groups (n =5/group) including control (Ctrl), ABT-199, Apatinib and combination (Comb), then treated for 2 consecutive weeks with vehicle (0.2% methyl cellulose and 0.1% Tween-80 in PBS), ABT-199 (80 mg/kg/day, oral gavage), Apatinib (100 mg/kg/day, oral gavage), or combined ABT-199 and Apatinib, respectively. (A)

Implementation scheme of in vivo experiment. (B) Tumor size. (C) During treatment, body weight of mice was monitored daily. (D, E) Tumor weight and volume. (F) Immunohistochemical staining for human CD45 was performed to examine infiltration of tumor cells (scale bar: 20 μm). (G) Western Blot analysis for p-VEGFR2, MAPK pathway associated proteins, BCL-2, and MCL-1 on tumor homogenate.

Figure 5

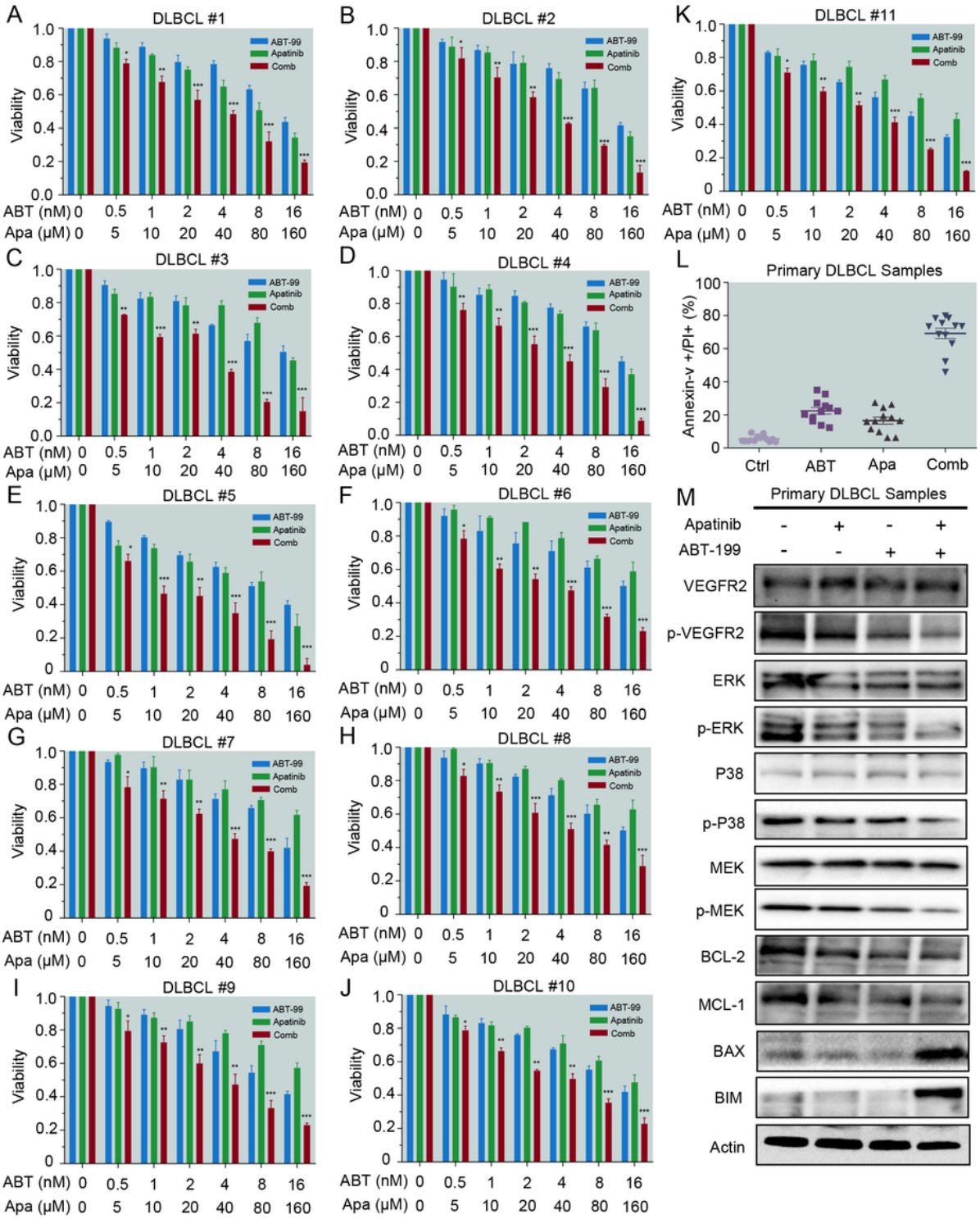

Figure 5

ABT-199 cooperates with Apatinib in killing primary DLBCL cells. Primary bone marrow cells and lymph node isolated from 5 DLBCL patients were treated with different concentrations of ABT-199 and Apatinib alone or in combination for 24 h. (A, B, C, D, E) Cell viability was measured by the CCK8 assay. Data are presented as mean ± SD; P values were calculated by the comparison between the combination group and ABT-199 or Apatinib alone group. (F) Primary blasts cells were exposed to the indicated concentrations of ABT-199 or Apatinib alone or in combination for 24 h, after which the percentage of Annexin-V+ apoptotic cells were determined by flow cytometry after Annexin-V and PI double staining. *P < 0.05, **P < 0.01, and ***P < 0.001.

Figure 6

Figure 6

DLBCL cells transcriptome determined by RNA sequencing. (A, B) Gene ontology (GO) analysis for differentially expressed genes treated with ABT-199 or Apatinib for 3 days (A UP genes, B DOWN genes). (C, D) Pathway analysis for differentially expressed genes from the DLBCL cells transcriptome (C UP genes, D DOWN genes). (E) Five KEY genes and Gene ontology (GO) activity network construction using cytoscape ($P < 0.05$). (F) GESA analysis of combination group using cytoscape ($P < 0.05$).

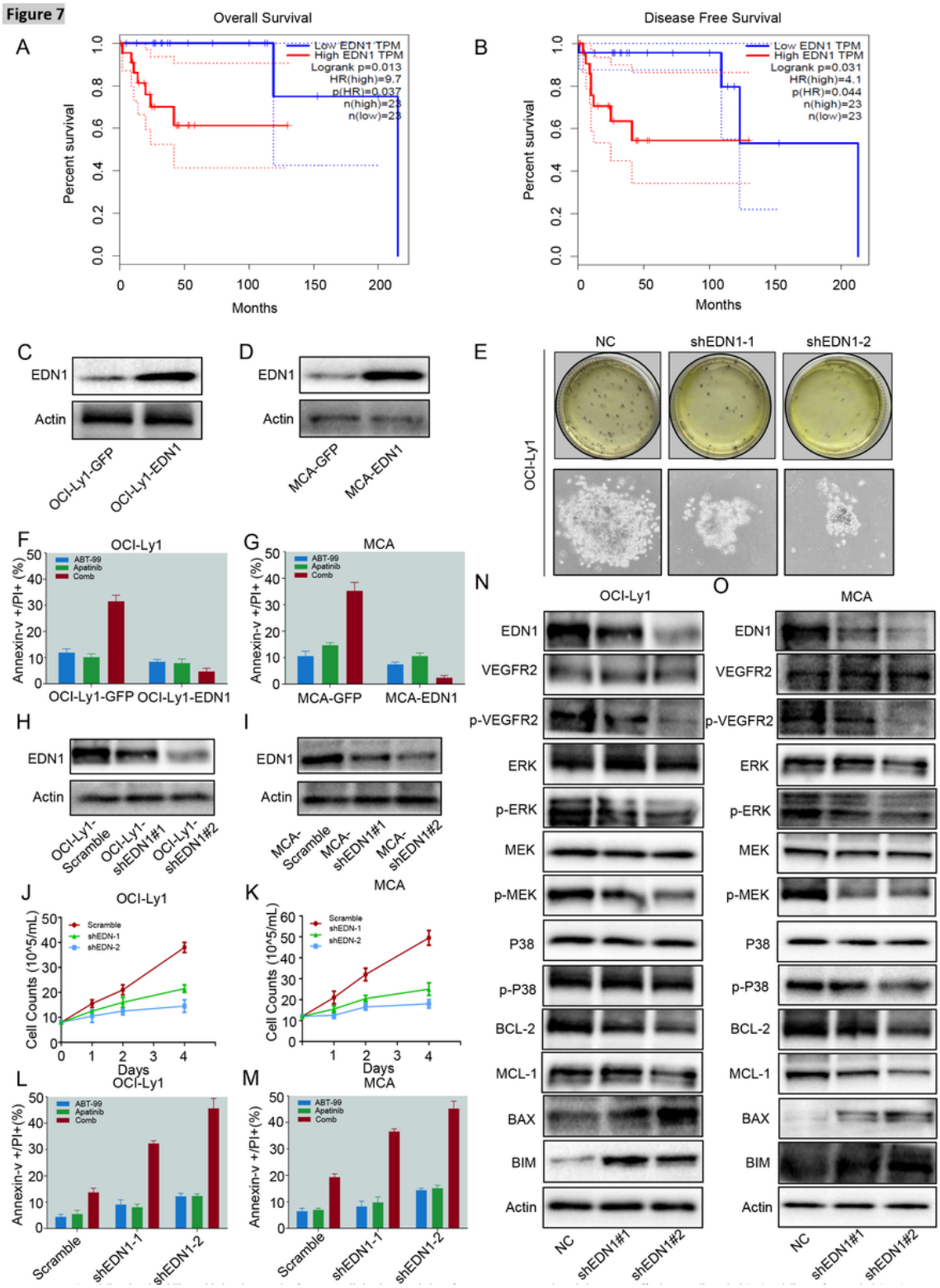

Figure 7

ABT-199/Apatinib reduced viability and induced apoptosis of DLBCL cells by downregulation of EDN1. (A, B) EDN1 is a vital oncogene affecting overall survival (OS) and disease-free survival (DFS). (C, D) EDN1 was overexpressing in OCI-Ly1 cells (left) and MCA (right). (F, G) OCI-Ly1 and MCA cells were treated with indicated concentrations of ABT-199 ± Apatinib for 24 h, after which the percentage of apoptosis was determined by flow cytometry. (E) When the EDN1 is knocked out the clonogenicity assay was performed

in OCI-Ly1 cells to determine the percentage of CFU. (H, I) Levels of EDN1 in OCI-Ly1 and MCA cells transduced with lentivirus vectors containing control shRNA (shNC), shRNA targeting EDN1 (shEDN1#1), or shEDN1#2 were detected by Western Blot analysis with antibodies indicated. (J, K) Proliferation of OCI-Ly1 and MCA cells expressing control and EDN1 shRNA were showed by counting viable cells about 3 days. (L, M) OCI-Ly1 and MCA cells were treated with indicated concentrations of ABT-199 ± Apatinib for 24 h, after which the percentage of apoptosis was determined by flow cytometry. (N, O) Levels of EDN1, p-VEGFR2, MAPK pathway associated proteins, anti-apoptosis BCL-2 and MCL-1 were detected by Western Blot analysis. Actin was used as a loading control after EDN1 knocked down.

Figure 8

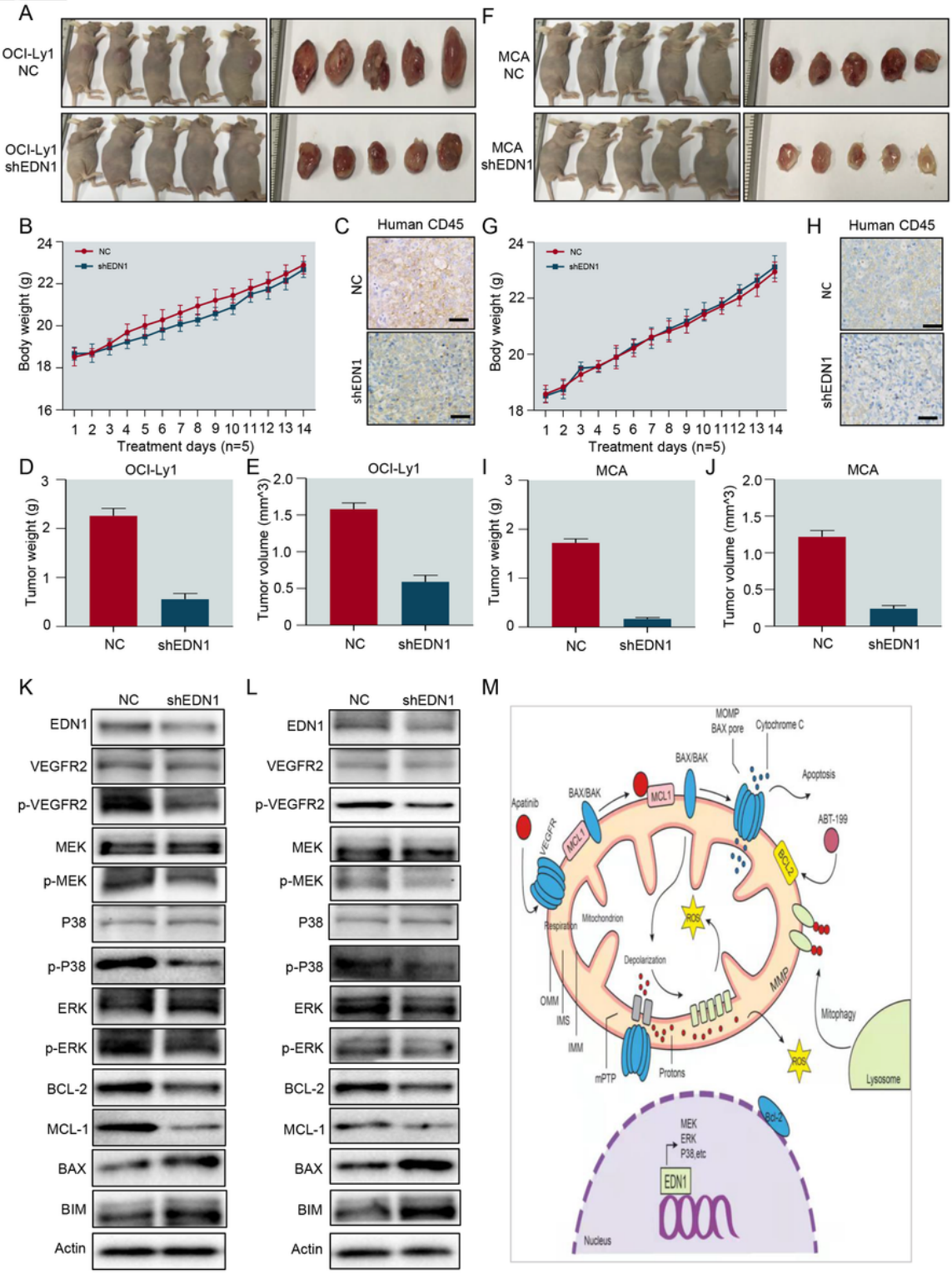

Figure 8

The EDN1 knocked down significantly reduce the tumor burden of BALB/C nude mice. (A, F) After the EDN1 was knocked down BALB/C nude mice were re-injected with OCI-Ly1 and MCA cells. Compared with the shNC, the tumor burden of mice was obviously inhibited after knocked down of EDN1. (B, G) During treatment, body weight of mice was monitored daily. (D, E, I, J) Tumor weight and volume. (C, H) Immunohistochemical staining for human CD45 was used to examine infiltration of tumor cells (scale

bar: 20 μm). (K, L) Western Blot analysis for EDN1, p-VEGFR2, MAPK pathway associated proteins, BCL-2, and MCL-1 on tumor homogenate. (M) Pharmacologic targeting EDN1 induces mitochondrial dysfunction, the decreased intracellular ROS levels and apoptosis in DLBCL.

Supplementary Files

This is a list of supplementary files associated with this preprint. Click to download.

- SupFigure1.pdf
- SupFigure2.pdf
- SupFigure3.pdf
- SupplememntalTable1.docx